Materials Letters 65 (2011) 1931–1934

Contents lists available at ScienceDirect

Materials Letters

journal homepage: www.elsevier.com/locate/matlet

Novel forsterite/polycaprolactone nanocomposite scaffold for tissue engineering applications

Mani Diba *, M.H. Fathi, M. Kharaziha

Biomaterials Group, Department of Materials Engineering, Isfahan University of Technology, Isfahan, 8415683111, Iran

ARTICLE INFO

Article history:
Received 6 October 2010
Accepted 12 March 2011
Available online 17 March 2011

Keywords:
Nanocomposites
Scaffold
Forsterite nanopowder
Porosity

ABSTRACT

Novel highly porous nanocomposite scaffolds consisting of polycaprolactone (PCL) and forsterite nanopowder were prepared by a solvent-casting/particle-leaching method. In addition, the effects of forsterite nanopowder contents on the structure of the scaffolds were investigated to provide an appropriate composite for bone regenerative medicine. Results showed that the scaffolds exhibited high porosity (up to 92%) with open pores of 100–300 μm average diameters. This porosity increased with decreasing forsterite nanopowder content. In addition, the pore walls contained numerous micropores. Microstructure studies showed that the pores were well distributed throughout the structures. Furthermore, the bioactive forsterite nanoparticles were homogenously distributed within the PCL matrix of the scaffolds, which contained up to 30 wt.% forsterite nanopowder. This porous structure with micropores provides the properties required for bone tissue engineering applications.

1. Introduction

A major goal of tissue engineering is to employ the principles of rational design to repair damaged tissues or produce new ones [1]. As porous structure implants allow tissue in-growth and vascularisation, they were studied extensively. Researchers need to address multiple biological, physical, and mechanical design constraints. For this reason, new types of biocompatible materials are regularly fabricated and characterized for medical applications. Taking into account that natural bone consists of organic and inorganic materials, significant attention is paid to polymer/ceramic composites [2–4].

Nanostructured Forsterite (Mg_2SiO_4) is a new bioceramic with good biocompatibility. Additionally, forsterite nanopowder, unlike micron-sized forsterite, is bioactive [5]. Researches show that forsterite has better mechanical properties than calcium phosphate ceramics, glasses and glass ceramics [6–9]. A few researches were performed on the fabrication and characterization of polymer-forsterite composites. In two researches, nanocomposites of PMMA-forsterite were prepared by two different methods [10,11]. However, these composites were not prepared for biomedical goals [10,11].

Another material of interest is polycaprolactone (PCL), a semi-crystalline polymer with good biocompatibility. Among all the bioresorbable polymers, it exhibits higher and more prolonged mechanical strength, and degrades at a compatible rate with bone regeneration [6,12,13]. It is predicted that a new material utilizing the mechanical properties and bioactivity of forsterite nanopowder combined with the biodegrability of PCL could result in a scaffold structure useful for bone tissue repair.

Several methods can be used for fabrication of scaffolds [14–18]. Solvent-casting/particle-leaching is one of the important methods for obtaining highly porous scaffolds. Sophisticated equipment is not required as the size and fraction of porosity are controlled by the initial size and fraction of porogen used. In this method, polymer is dissolved in an organic solvent, and then mixed with ceramic granules and salt particles. After casting the solution into a predefined 3D mold, the solvent evaporates and salt particles are leached out by water to generate the interconnected pores [12,19].

In this investigation, novel 3D porous nanocomposite scaffolds made of forsterite nanopowder and PCL were developed for bone tissue engineering. They were fabricated by the solvent-casting/particle-leaching method. In addition, the effects of forsterite nanopowder contents on the structures of scaffolds were investigated.

2. Experimental methods

2.1. Preparation of nanocomposite scaffolds

The forsterite nanopowder/PCL composite scaffolds were prepared by a solvent-casting/particle-leaching method using NaCl particles as the porogen. The forsterite nanopowder with particle size in the range of 25–45 nm was prepared according to the sol–gel process described in our previous report [5]. The PCL was supplied as pellets (Molar weight in range of 70,000–90,000 g/mol) and NaCl sieved particles (Sodium chloride extra pure) had a particle size of 250–297 μm. Five types of

* Corresponding author. Tel.: +98 9131 1232294; fax: +98 9131 8525245.
E-mail addresses: manidiba@gmail.com, Mani.Diba@map.stud.uni-erlangen.de (M. Diba).

0167-577X/$ – see front matter © 2011 Elsevier B.V. All rights reserved.
doi:10.1016/j.matlet.2011.03.047

Table 1
Preparation parameters and porosities of the neat polymer and nanocomposite scaffolds.

Sample	Forsterite (wt.%)	PCL (wt.%)	NaCl (wt.%)[a]	Porosity (%)
1	0	100	80	92.65
2	10	90	80	92.14
3	20	80	80	91.86
4	30	70	80	91.38
5	40	60	80	91.03
6	50	50	80	90.94

[a] The percentage of NaCl is to the total weight of PCL and forsterite nanopowder.

porous PCL nanocomposites containing 10, 20, 30, 40 and 50 wt.% of forsterite nanopowder were synthesized. In order to prepare the composite scaffolds, PCL pellets were dissolved in Chloroform with a concentration of 0.1 g/ml and then fixed amounts of forsterite nanopowder were added into the solution while continuously stirring. The weight percentages of the PCL, forsterite nanopowder, and NaCl are shown in Table 1. After a complete dispersion of the forsterite nanopowder, NaCl particles were added into the suspension and the final dispersion was casted into cylindrical Teflon molds. The samples were air-dried for 48 h to allow the solvent to evaporate completely. In order to leach the salt particles out, the samples were soaked in deionized water for 3 days. The water was replaced three times by fresh water during this period. Salt-removed samples were freeze-dried, and porous composite scaffolds were obtained and stored under vacuum until they were used for testing. In order to make a comparison, a neat polymer scaffold was prepared without forsterite nanopowder.

2.2. Characterization of nanocomposite scaffolds

The structural morphology of the neat PCL scaffold and the nanocomposite scaffolds were examined using scanning electron microscope (SEM), EDS and X-ray map techniques. The FTIR spectra of the neat PCL and nanocomposite scaffolds were characterized using a FTIR spectrometer. The phase analysis was carried out by X-ray diffraction (XRD) technique. The porosity of the scaffolds was calculated by Archimedes' method. The porosities were calculated using the following equations:

$$V_{s_1} = \frac{[W_1-(W_2-W_s)]}{\rho} \quad (1)$$

$$Porosity(\%) = \left(1-\frac{V_{s_1}}{V_{s_2}}\right) \times 100 \quad (2)$$

Where V_{s1} is the volume of the scaffold, W_1 is the weight of the gravity bottle filled with ethanol, W_2 is the weight of the gravity bottle filled with ethanol and the immersed scaffold, W_s is the weight of the scaffold, is the density of ethanol, V_{s2} is the volume of the entire scaffold.

3. Results and discussion

Fig. 1 shows the SEM micrographs of the surfaces of the neat polymer and nanocomposite scaffolds. The neat PCL scaffold is characterized by a highly macroporous structure. The pores are interconnected and their sizes varied from 100 to 400 μm (Fig. 1a). Rougher and less regular scaffold structures were observed on surfaces prepared in the presence of forsterite. The measured porosity percentages of the neat PCL and nanocomposite scaffolds are presented in Table 1. As can be seen, the porosities decrease with increasing forsterite contents. The open pores are about 100–300 μm in size. Furthermore, thicker walls and a more uneven structure than that of the neat polymer scaffold were observed on composite scaffolds. The scaffolds not only have macropores, but also plentiful micropores (on the scale of 1–10 μm) on the macroporous walls.

This structure fulfills all of the porosity criteria for an ideal scaffold. These micropores may appear during the fabrication due to the porogen cleavage and/or due to the grains, which are not located in the same plain as the majority of porogen crystals. Research showed that, for the migration and proliferation of osteoblasts cells, the presence of these open and interconnected pores are necessary in bone tissue engineering

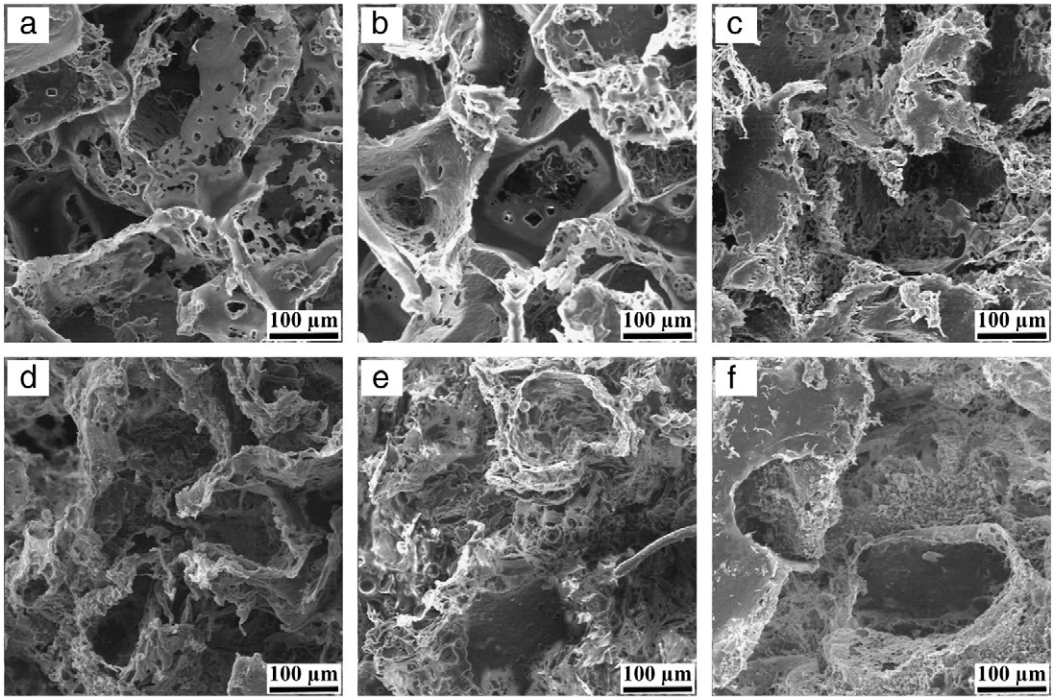

Fig. 1. SEM image of surface morphology of (a) the neat PCL, (b) the PCL-10 wt.% forsterite, (c) the PCL-20 wt.% forsterite, (d) the PCL-30 wt.% forsterite, (e) the PCL-40 wt.% forsterite, and (f) the PCL-50 wt.% forsterite scaffolds.

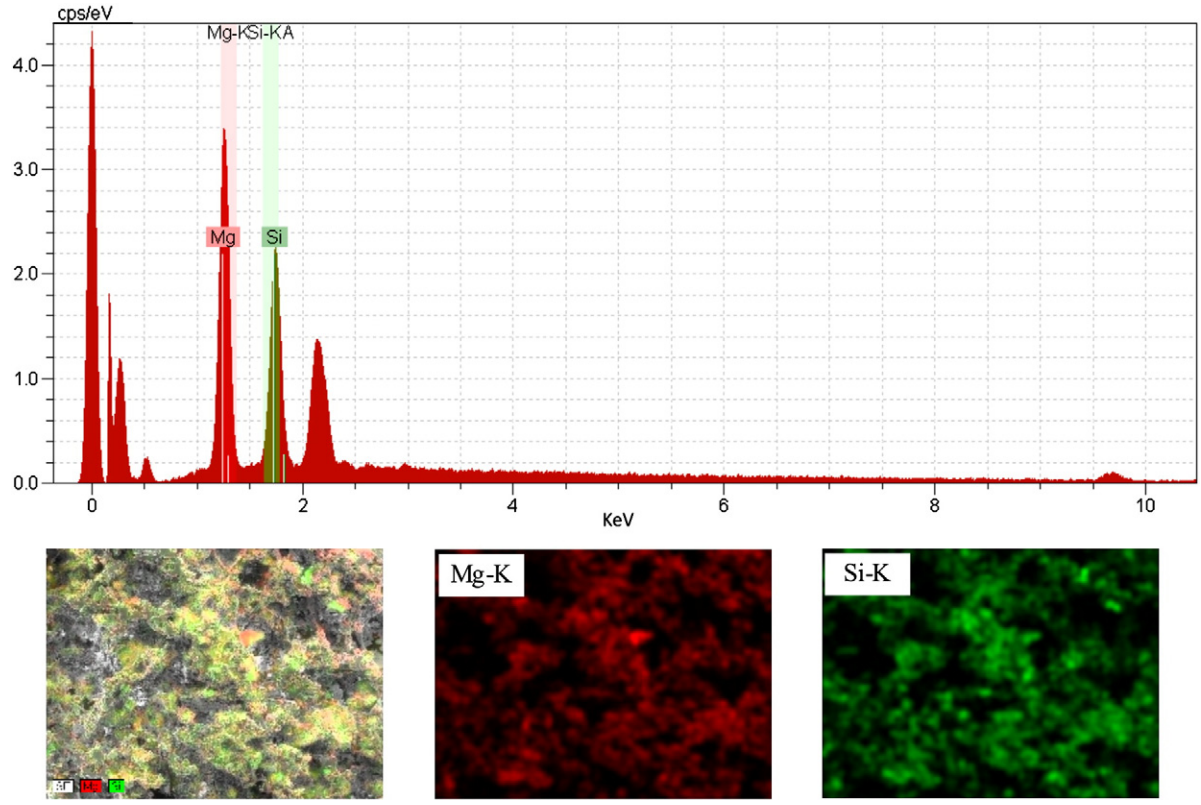

Fig. 2. The EDS spectrum and X-ray map of the PCL-30 wt.% forsterite scaffold.

[2]. In the presence of 10 wt.% forsterite nanopowder, the macroporous structure was similar to that of the neat PCL scaffold. It also showed that at a low content of forsterite nanopowder (up to 10 wt.%), the forsterite particles did not perturb the solvent crystallization to a large extent. The SEM micrographs of nanocomposite scaffolds showed that the scaffolds which contain up to 30 wt.% forsterite nanopowder have the steady porosities, and their pores are open and interconnected. Samples with higher amounts of forsterite (up to 40 wt.%) still maintained the macroporous structure in the scaffold, but suffered from inferior pore interconnectivity and even displayed residual forsterite aggregates (Fig. 1e).

Fig. 2 shows the EDS spectrum and X-ray map of the nanocomposite scaffold containing 30 wt.% forsterite nanopowder. The EDS spectrum shows the peaks of Mg and Si with Mg/Si = 2 which is supporting the presence of forsterite particles. Furthermore, as can be seen in the map, forsterite particles are dispersed on the pore surfaces without any agglomeration. Moreover, the forsterite particles are observed both on the pore surfaces and embedded in the walls of the composite scaffolds.

Increased percentages of forsterite nanoparticles resulted in some degradation of the porosity of scaffold structure. Still, some forsterite nanoparticles are necessary to provide good bioactivity for the structure and improved mechanical properties [5]. It is expected that an optimum percentage of forsterite nanoparticles could be discovered, which provides these desirable attributes without significantly impacting the overall porosity of the structure.

W. Cheng et al. [3] reported that the addition of h-Ca_2SiO_4 in the PDLLA matrix, results in a decrease of the porosity, the aggregation of the ceramic particles and also more ceramic particles at the surface of pore walls. Jin et al. [4] reported, with increasing of the ceramic amount, the porosity and average pore size decreased, the pore structure locally collapsed and appeared to be agglomerated.

The XRD patterns of the forsterite nanopowders, neat PCL and nanocomposite scaffolds which contain 20 and 40 wt.% of forsterite

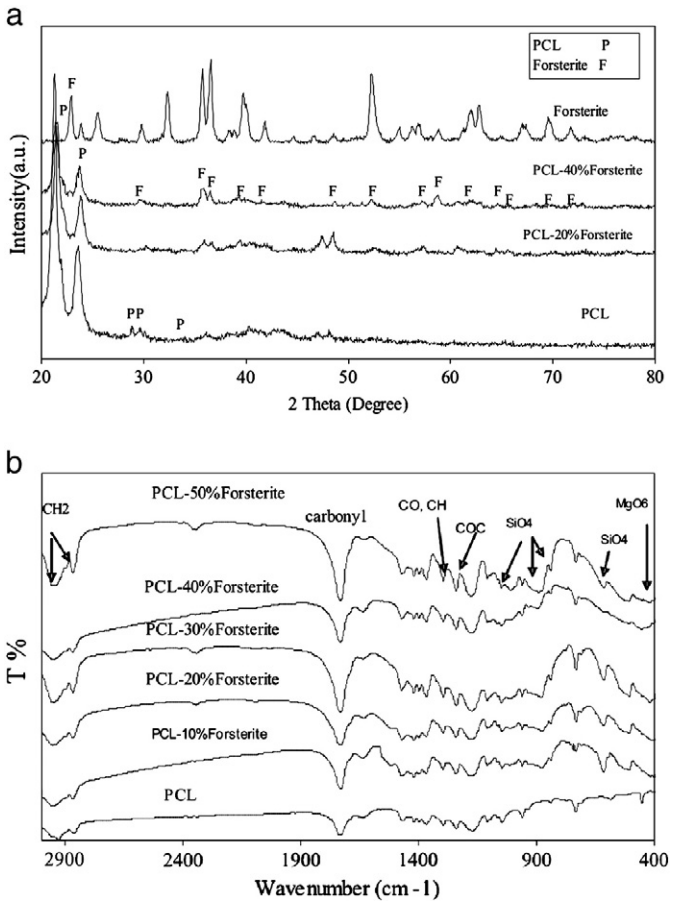

Fig. 3. (a) XRD patterns and (b) FTIR spectra of the neat PCL, forsterite nanopowder, and nanocomposite scaffolds.

nanopowder are depicted in Fig. 3a. The neat PCL scaffold pattern contains only the PCL characteristic peaks. The XRD patterns of the nanocomposite scaffolds exhibited peaks from both materials; forsterite and PCL. Besides showing weakened PCL peaks, characteristic peaks of forsterite were also observed. Increasing the forsterite to 40 wt.% resulted in more intensive forsterite peaks. In addition, the weak peaks of PCL had disappeared.

Fig. 3b shows the FTIR spectra of the neat PCL and nanocomposite scaffolds. These spectra reveal the presence of characteristic PCL-related stretching modes in the PCL and nanocomposite scaffolds. These include 2949 cm^{-1}, and 2865 cm^{-1} (symmetric CH_2 stretching), 1727 cm^{-1} (carbonyl stretching), 1293 cm^{-1} (C—O and C—C stretching in the crystalline phase) and 1240 cm^{-1} (asymmetric COC stretching) [20]. In addition, the spectra of nanocomposites revealed the presence of characteristic bands for the forsterite, with the peak at 830–1000 cm^{-1}, 500–620 cm^{-1} being to the silicate group and at 475 cm^{-1} being to the MgO_6 [21].

4. Conclusions

The novel highly porous nanocomposite scaffolds which consisted of forsterite nanopowder and PCL were fabricated using a solvent-casting/particle-leaching method. Using forsterite nanopowders as the bioactive and reinforcement agent, the series of characteristic interconnected open pore microstructures with the porosities about 90–92.5% were fabricated. Results show that the optimum percentage of forsterite nanopowder that provides the most suitable morphology is 30 wt.%, which shows a steady dispersion of forsterite nanopowder in their structures. However, the scaffolds which contain a higher amount of forsterite nanopowder lack a steady dispersion of forsterite nanopowder and with higher than 40 wt.% also lack sufficient porosity and pore interconnectivity. This porous nanocomposite scaffold exhibits enough porosity and pore interconnectivity to make it a good candidate for bone tissue engineering applications.

Acknowledgments

The authors are grateful for the support of this research by the Isfahan University of Technology. We also thank Keith Thomas for his kind help.

References

[1] Fisher JP, Mikos AG, Bronzino JD. Tissue Engineering. CRC press; 2006.
[2] Hutmacher DW. Biomaterials 2000;21:2529–43.
[3] Cheng W, Li H, Chang J. Mater Lett 2005;59:2214–8.
[4] Jin HH, Lee CH, Lee WK, Lee JK, Park HC, Yoon SY. Mater Lett 2008;62:1630–3.
[5] Kharaziha M, Fathi MH. Ceram Int 2009;35:2449–54.
[6] Rezwan K, Chen QZ, Blaker JJ, Boccaccini AR. Biomaterials 2006;27:3413–31.
[7] Hench LL. Bioceramics J Am Ceram Soc 1998;81:1705–33.
[8] Suchanek W, Yoshimura M. J Mater Res 1998;13:94–117.
[9] Ducheyne P. J Biomed Mater Res 1987;21:219–36.
[10] Kang J, Park SH, Kwon HY, Park DG, Kim SS, Kweon HJ, et al. Bull Korean Chem Soc 1998;19:503–6.
[11] Park DG, Kang J, Kwon HY. Bull Korean Chem Soc 2000;21:604–10.
[12] Gunatillake PA, Adhikari R. Eur Cell Mater 2003;5:1–16.
[13] Fabbri P, Bondioli F, Messori M, Bartoli C, Dinucci D, Chiellini F. J Mater Sci Mater Med 2010;21:343–51.
[14] Reignier J, Huneaulta MA. Polymer 2006;47:4703–17.
[15] Jiang T, Abdel-Fattah WI, Laurencin CT. Biomaterials 2006;27:4894–903.
[16] Liulan L, Qingxi H, Xianxu H, Gaochun X. J Rare Earths 2007;25:379–83.
[17] Chen QZ, Thompson ID, Boccaccini AR. Biomaterials 2006;27:2414–25.
[18] Roether JA, Boccaccini AR, Hench LL, Maquet V, Gautier S, Jerome R. Biomaterials 2002;23:3871–8.
[19] Khang G, Suk Kim M, Bang Lee H. Manuals in biomedical research. A manual for biomaterials/scaffold fabrication technology, vol. 4. World Scientific Publishing Co. Pte. Ltd; 2007.
[20] Catledge SA, Clem WC, Shrikishen N, Chowdhury S, Stanishevsky AV, Koopman M, et al. Biomed Mater 2007;2:142–50.
[21] Fathi MH, Kharaziha M. J Alloy Compd 2009;472:540–5.